Limnol. Oceanogr., 51(6), 2006, 2621–2631

Zooplankton retention in the estuarine transition zone of the St. Lawrence Estuary

Rachel D. Simons[1] *and Stephen G. Monismith*
Civil and Environmental Engineering, Stanford University, Stanford, California 94305

Ladd E. Johnson and Gesche Winkler
Biology Department, Laval University, Quebec, Quebec G1K 7P4, Canada

François J. Saucier
Division of Ocean Sciences, Maurice Lamontagne Institute, Department of Fisheries and Oceans, Mont-Joli, Quebec G5H 3Z4, Canada

Abstract

We used a three-dimensional physical–biological model consisting of a Eulerian circulation model and a Lagrangian particle-tracking model, which included vertical sinking and swimming, to explore zooplankton retention in the estuarine transition zone of the St. Lawrence Estuary (SLETZ). To test the accuracy of the model, the results were temporally and spatially compared to a passive scalar released simultaneously in the circulation model and to field data for zebra mussel veligers. The model was then used to study the effects of baroclinic density-driven flow, vertical sinking and swimming, and tidal vertical migration on retention of simulated zooplankton. Baroclinic flow, created by longitudinal and lateral salinity gradients, was a critical part of retention in the SLETZ. In the presence of baroclinic flow, vertical sinking and swimming speeds of ≥ 0.2 mm s^{-1} had a large effect on the residence time of the simulated zooplankton as a result of gravitational circulation. Tidal vertical migration—a pattern of upward movement on flood and downward movement on ebb—was a viable retention mechanism for the SLETZ, and its effectiveness was amplified by baroclinic flow. As the speed of tidal vertical migration increased, the simulated zooplankton were concentrated in smaller areas of the SLETZ and moved further upstream.

In coastal plain estuaries, the estuarine transition zone (ETZ) occurs where freshwater from the river mixes with the salt water from the estuary and is characterized by well-defined salinity gradients and long residence times. High concentrations of zooplankton biomass and suspended sediment are observed in the ETZ (Kimmerer et al. 1998; Roman et al. 2001), which is also called the estuarine turbidity maximum. With a constant river flow, the depth-averaged residual or mean current in the ETZ is downstream and seaward (Kimmerer et al. 1998). Yet it has been well documented that stable populations of zooplankton, often associated with a specific salinity zone, live and thrive in the ETZ (Miller 1983; Laprise and Dodson 1994; Winkler et al. 2003), indicating that physical and biological mechanisms allow the zooplankton to maintain their position in the ETZ (Kimmerer et al. 1998, 2002).

The task of remaining in the ETZ is particularly challenging for zooplankton in the St. Lawrence Estuary, one of the largest and most energetic estuaries in North America and the study area for this project (Fig. 1). The energy in the St. Lawrence Estuary derives from tides that have tidal ranges of up to 10 m and tidal currents of up to 3 m s^{-1} (Mertz and Gratton 1990) and from the St. Lawrence River that has an average discharge of 11,900 m^3 s^{-1} (El-Sabh and Silverberg 1990). The downstream residual currents in the estuarine transition zone of the St. Lawrence Estuary (SLETZ) are estimated to range up to 50 cm s^{-1} (Simons 2004). In spite of the large river flow, stable zooplankton assemblages occur in the SLETZ in specific salinity zones (Bousfield et al. 1975; Laprise and Dodson 1994).

A physical mechanism that could promote retention for the SLETZ is density-driven baroclinic flow, which is created by horizontal salinity gradients and the residuals of which, called gravitational circulation, counterbalance the net downstream flow. In some estuaries, gravitational circulation takes the form of two-layer exchange flow, which is a mean pattern of upstream bottom flow and downstream surface flow (Fischer et al. 1979). The height at which this mean exchange flow equals zero is called the level of no motion (Dyer 1997). The location at which the level of no motion reaches the bed, called the null point, has

[1] To whom correspondence should be addressed. Present address: East Bay Municipal Utility District, 375 11th Street, MS 901, Oakland, California 94607 (rsimons@ebmud.com).

Acknowledgments

We thank the following organizations for their support of this project: Stanford University UPS grants, the National Science Foundation graduate research fellowship program, the American Association of University Women Educational Foundation selected professions fellowships, the U.S. Environmental Protection Agency National Center for Environmental Research STAR graduate fellowships (grant U91623201), and the Canadian National Science and Engineering Research Council (NSERC Strategic Grant 224180). The assistance of the Ocean Sciences Division, Maurice Lamontagne Institute, Fisheries and Oceans Canada, with model development was greatly appreciated. We also thank Christine Barnard, for providing us with veliger data for the fixed station, as well as Julian J. Dodson.

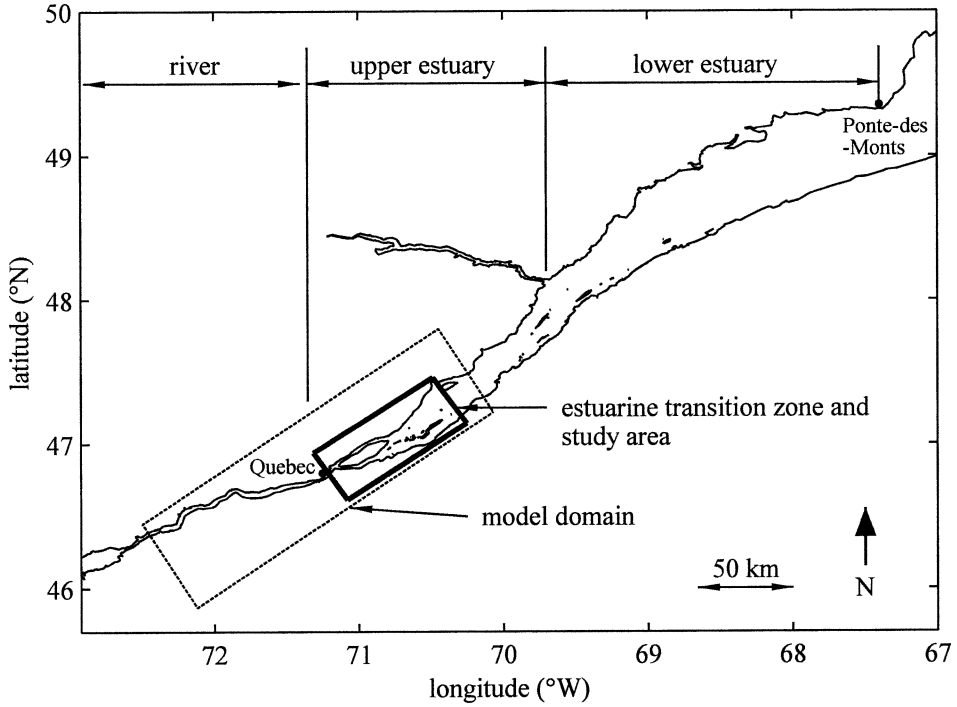

Fig. 1. St. Lawrence River and Estuary with model domain and estuarine transition zone/ study area.

been hypothesized to contain zooplankton and suspended sediment in the ETZ (Arthur and Ball 1979; Morgan et al. 1997). However, residual circulation in the ETZ is usually not this straightforward as a result of variability in river flow and bathymetry (Kimmerer et al. 1998; Monismith et al. 2002).

A biological retention mechanism that could promote retention for the SLETZ is tidal vertical migration (TVM), which is also called selective tidal stream transport. Zooplankton use TVM to maintain their position in an estuary by migrating up to the surface on flood and down to the bottom on ebb (Cronin and Forward 1982; reviewed by Forward and Tankersley 2001). TVM allows the zooplankton to overcome the net seaward flow by taking advantage of the fast upstream currents near the surface on flood and the slow downstream currents near the bed on ebb (Kimmerer et al. 1998). TVM has been observed for many different types of zooplankton, such as fish larvae, copepods, and mysids (Morgan et al. 1997; Kimmerer et al. 1998; Grioche et al. 2000), and specifically for larval rainbow smelt, *Osmerus mordax*, in the SLETZ (Laprise and Dodson 1989; Dauvin and Dodson 1990).

In this study, we used a three-dimensional physical–biological model to explore zooplankton retention in the SLETZ. The physical–biological model consisted of two parts, a Eulerian circulation model and a Lagrangian particle-tracking model. Because of their slow swimming rates, which are typically on the order of millimeters per second (Young 1995), zooplankton can only control their movement vertically in the ETZ. To accommodate vertical zooplankton movement, a biological velocity, which represents vertical swimming and sinking, was incorporated into the particle-tracking model. The combined Eulerian–Lagrangian model, also known as an individually based model, is useful because an individual particle can be provided with its own physiology and behavior and because population dynamics can be simulated (Batchelder et al. 2002). Physical–biological models have been successfully used to study the transport of many types of zooplankton, such as copepods (Hannah et al. 1997; Harms et al. 2000; Batchelder et al. 2002), veligers (Tremblay et al. 1994), and fish larvae (Bartsch 1993; Hare et al. 1999). Our study differs from previous work in examining the effects of baroclinic density-driven flow on zooplankton retention and retention mechanisms.

For our study, the physical–biological model was first verified by comparing particle results to a passive scalar released simultaneously in the circulation model. Next, particle results were compared to field data for zebra mussel larvae in a case study. Once the model was tested, the physical and biological retention mechanisms of baroclinic flow, vertical swimming and sinking, and TVM were examined and the following questions explored: How do baroclinic flow and vertical particle motion affect the distribution and residence times of particles in the SLETZ? What is the relationship between vertical particle motion and baroclinic flow? Is TVM a viable retention mechanism for zooplankton in the SLETZ? We begin with a description of the physical–biological model, its verification, and a case study. We then report methods and results for each modeling exercise that address the questions posed.

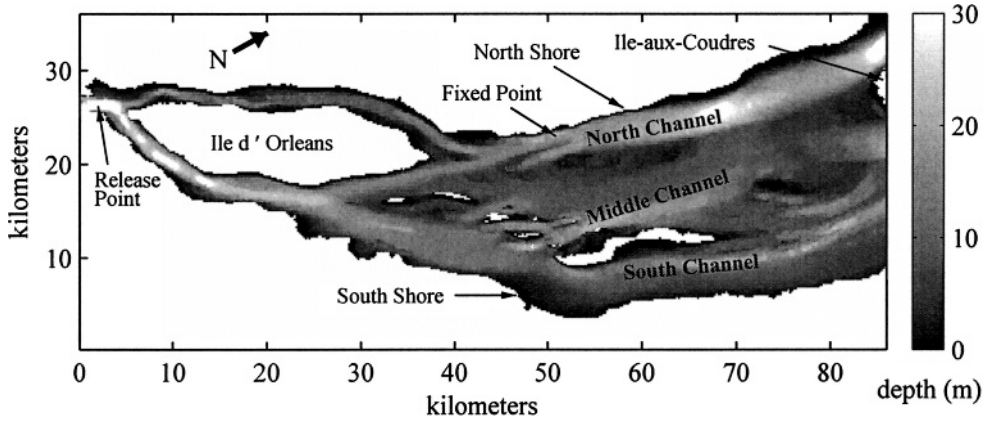

Fig. 2. Bathymetry of the estuarine transition zone and study area. Particles were introduced into the model domain at the release point. Zebra mussel veligers were collected at the fixed point.

Physical–biological model

Zooplankton retention in the SLETZ was explored using a three-dimensional physical–biological model that comprised a Eulerian circulation model and a Lagrangian particle-tracking model. The velocities and vertical eddy diffusivities produced by the circulation model drove the particle-tracking model, which in turn created three-dimensional particle trajectories. The advantages of using a Lagrangian particle-tracking model for zooplankton transport rather than a Eulerian model were that the particles could be tracked within a grid cell and that biological responses, such as swimming, could be imposed on individual particles (Hoffmann and Lascara 1998). The following sections describe the methods used for the circulation and particle-tracking models.

Circulation model—The circulation model used in this study was the three-dimensional hydrodynamic model Tidal, Residual, Intertidal Mudflat 3D, or TRIM3D (Casulli and Cheng 1992; Casulli and Cattani 1994). The governing equations for TRIM3D are the Reynolds averaged Navier–Stokes equations with the assumptions of hydrostatic flow, incompressibility, and the Boussinesq approximation. A square staggered grid is used to define all properties. The QETE turbulence closure model, which is a modification of the Mellor–Yamada level 2.5 model, and the scalar transport were added to TRIM3D by Gross et al. (1999). The TRIM3D model simulates both tidal barotropic and density-driven baroclinic flows.

The locations of the model domain and study area, which contain the SLETZ, are shown in Fig. 1. The model domain was rotated 46° from latitude to align the x-direction with the longitudinal river flow. The model's grid had 1,049 by 330 points with 200-m spacing in the horizontal plane and 41 points with 2-m spacing in the vertical plane. With this grid spacing, the model had a total of 49,748 two-dimensional water columns and 412,147 three-dimensional active grid points. The bathymetry of the SLETZ and study area includes a width that varies from 2 to 24 km, deep channels, islands, and shallow shoals (Fig. 2) (Mertz and Gratton 1990).

Currents in the circulation model were driven by river and tidal flow. The freshwater inflow from the St. Lawrence River was specified at the upstream boundary of the model domain and ranged from approximately 7,500 $m^3\ s^{-1}$ to 9,000 $m^3\ s^{-1}$ over the modeling period. Tidal flow and salinity were introduced at the downstream boundary of the model domain. The modeling period for this study covered 58 d from 14 July to 09 September 2001. All simulations were run with a 180-s time step. A detailed description of the application of TRIM3D to the SLETZ, including boundary conditions, initial conditions, and calibration to field observations, is presented in Simons (2004).

Particle-tracking model—The particle-tracking model used the Lagrangian form of the advection–diffusion equation with a random-walk method for transport by turbulent diffusion. Since horizontal eddy diffusivities in the circulation model were set to zero, particle movement in the horizontal x–y plane was represented by Eqs. 1 and 2, thus:

$$\Delta x = u\Delta t \tag{1}$$

$$\Delta y = v\Delta t \tag{2}$$

where $u(x, y, z, t)$ = velocity in the horizontal x-direction; $v(x, y, z, t)$ = velocity in the horizontal y-direction; and Δt = time step. In the vertical direction, the circulation model produced spatially varying vertical eddy diffusivities, so a more complex version of the random walk method was needed. The following equations that separate vertical particle movement into three steps were used for vertical transport (Visser 1997; Batchelder et al. 2002):

$$z_o = z_n + (w + w_b)\Delta t \tag{3}$$

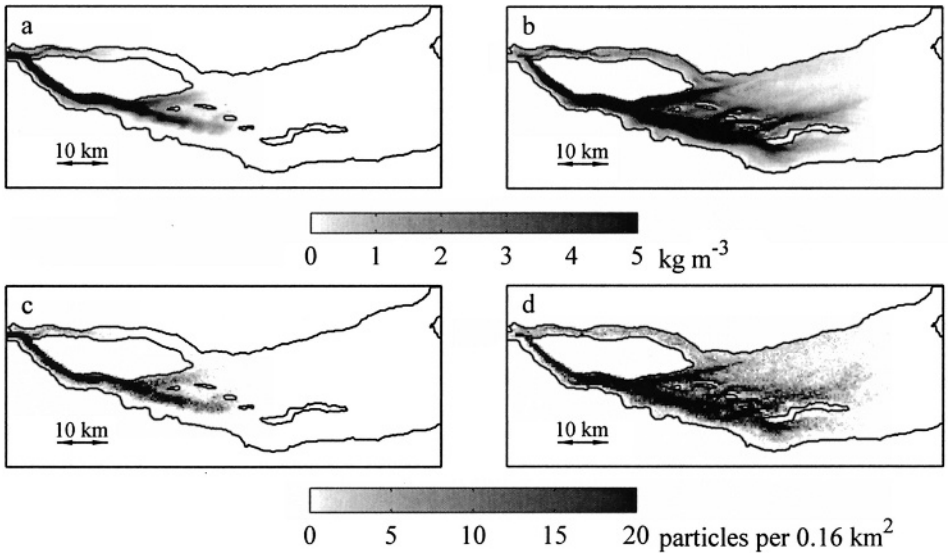

Fig. 3. Depth-averaged passive scalar concentrations after (a) 2.2 d and (b) 5.6 d. Distributions of passive particles after (c) 2.2 d and (d) 5.6 d.

$$z^* = z_0 + \frac{\partial \varepsilon_z}{\partial z}(z_o)\Delta t \tag{4}$$

$$z_{n+1} = z^* + Z\sqrt{2\varepsilon_z\left(\frac{1}{2}(z_0 + z^*)\right)\Delta t} \tag{5}$$

where $w(x, y, z, t)$ = velocity in the vertical z-direction; w_b = biological velocity; ε_z (x, y, z, t) = eddy diffusivity in the vertical z-direction; n = time step; and Z = an independent random number with a normal distribution, a zero mean, and a unit variance (Ahrens and Dieter 1973). Equations 3 through 5 include probability and momentum statistics for a spatially varying field of eddy diffusivity (Thomson 1984; Okubo 1986; Hunter et al. 1993). Biological velocity, w_b, represented the zooplankter's vertical movement as a result of swimming or sinking. In this article, upward swimming was defined as a positive biological velocity and downward swimming or sinking as a negative biological velocity. Biological velocities were not included in the horizontal transport equations because horizontal swimming speeds of zooplankton are usually orders of magnitude smaller than the horizontal currents in the ETZ and thus have no effect on their horizontal transport (Young 1995).

Trilinear interpolation was used to determine the velocities and vertical eddy diffusivities at the particle location within a grid cell. The vertical gradient of eddy diffusivity was determined by calculating the gradients with a first-order forward difference in space at the surrounding grid points and then by trilinearly interpolating the gradient at the particle location. To update the particle position by advection and biological velocity, fourth-order Runge–Kutta integration was used.

Horizontal and vertical boundary conditions were selected that would allow the particles to remain in the water column. For the surface and bottom boundaries, the surface height and water column depth were first bilinearly interpolated at the particle location. If the particle moved beyond these boundaries, it was reflected back into the water column. For the horizontal boundary, since the exact location of the shoreline was not known, the particles were reflected off the side of the first land grid cell. At certain locations near the shoreline, horizontal velocities for a particle were calculated at zero as a result of the staggered grid used in TRIM3D, even though the particle was still in the water column and had not moved beyond the horizontal boundary. In these cases, the horizontal velocities were trilinearly interpolated using a block of four grid cells to keep the particle moving. When a particle reached the upstream and downstream boundaries of the model domain, it was removed from the simulation. For this study, the particles never reached the upstream boundary, since they were released 110 km downstream.

For accuracy in particle-tracking models, the particles must not move more than one grid cell per time step. This criterion is based on the dimensionless Courant number, for which the following conditions must hold true; $\frac{u\Delta t}{\Delta x} \leq 1$, $\frac{v\Delta t}{\Delta y} \leq 1$, and $\frac{w\Delta t}{\Delta z} \leq 1$, where Δx is the distance moved in the x-direction, Δy is the distance moved in the y-direction, and Δz is the distance moved in the z-direction (Ferziger 1998). To meet the Courant number criterion, the time step of the particle-tracking model had to be subcycled to a 60-s time step from the circulation model time step of 180 s, allowing most of the particles to move one grid cell per time step.

Model verification

To test the accuracy of the physical–biological model, the particle-tracking results for passive or neutrally buoyant particles were compared to a passive scalar simulated by the circulation model. The passive scalar comparison mimicked a dye-release field experiment. If the

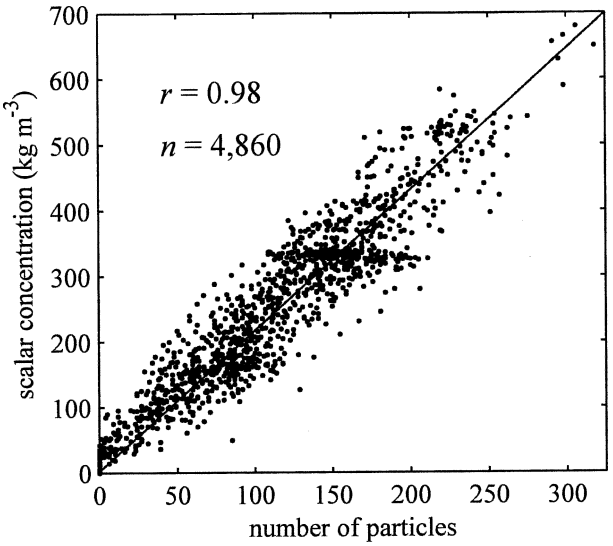

Fig. 4. Scalar concentration versus number of particles for 23 August 2001 at 06:00 h.

physical–biological model was accurate, the passive particles should evolve similarly in time and space as the passive scalar. The particles and scalar were introduced simultaneously into the model at the release point (Fig. 2), near the upstream boundary of the study area, and were released continuously at a rate of 20 particles per time step and 20 kg per time step, respectively, over the course of the modeling period. The upstream release point was selected so that the particles and scalar would be transported through the length of the study area. This release point was used for all simulations presented in this article. At the release point, both the scalar and the particles were evenly distributed at 2-m intervals over depths of 8–46 m. To create the same conditions as the particles, the scalar was removed from the domain when it reached the upstream or downstream boundary.

The particles and scalar showed good spatial and temporal agreement for horizontal and vertical distributions. The horizontal distributions of scalar and particles, respectively, at 2.2 d and 5.6 d from the start of release are displayed (Fig. 3). The scalar distribution is presented in depth-integrated concentrations. The particle distribution is represented by the total number of particles in the water column over four horizontal grid cells, an area of 0.16 km^2 (a convention used throughout this article). The vertical distribution of particles and scalar were examined throughout the study area and found to be evenly distributed throughout the water column. However, the vertical particle concentrations had random variations when compared to the homogeneous vertical scalar concentrations; these variations were likely caused by the limited number of particles released as a result of computational constraints.

For a statistical comparison, correlation coefficients of scalar and particle concentrations were calculated at 3-h intervals for the last 18 d of the simulation period, from 23 August to 09 September. The number of particles and scalar concentration summed over an area of 0.64 km^2, 16 grid cells, were compared. For example, the number of particles versus the scalar concentration on 23 August at 06:00 h is shown in Fig. 4. The correlation coefficients (r) calculated in this manner ranged from 0.95 to 0.98, with a mean value of 0.97.

The residence times of the scalar and particles were also compared. Once a system has reached a dynamic steady state, the residence time (T_{res}), also called flushing time, can be approximated by the following equation (Fischer et al. 1979):

$$T_{res} = \frac{M}{M^*} \tag{6}$$

where M is the total mass in the system and M^* is a constant discharge rate. The residence time, T_{res}, represents the average time a particle or 1 kg of mass remains in the system. To calculate the residence time, the mass or number of particles was averaged over the last fortnightly spring-neap cycle of the modeling period from 25 August to 09 September 2001. Using this method, the residence time was estimated to be 14.8 d for the particles and 13.1 d for the scalar.

Although the correlation coefficients and residence times showed good agreement between the scalar and the particle results, the differences were likely due to two factors: the inexact nature of the horizontal boundary condition, which could cause the particles to become trapped near the shoreline, slowing down their travel times, and the difference between the circulation and particle-tracking models in terms of their treatment of intertidal wetting and drying. In the particle-tracking model, if a particle was transported into an exposed mudflat or dry cell, it would remain there until the next tidal cycle brought it back into the water column, while in the circulation model, the scalar could only move into cells that are wet. Although these factors may be sources of error in the particle-tracking model, they are not believed to affect the conclusions presented in this article.

Case study: zebra mussel veligers

A recent invader to the SLETZ, zebra mussel larvae, know as veligers, are advected into the SLETZ from the St. Lawrence River (Winkler et al. 2005). In early summer, veligers numerically dominate the freshwater zooplankton assemblage, located in the freshwater upstream of Ile d'Orleans (Fig. 2), and the true estuarine zooplankton assemblage, located between Ile-aux-Coudres and Ile d'Orleans (Fig. 2) in salinities from 0.5 to 5 (Winkler et al. 2005). The abundance of veligers is largely controlled by advection from populations upstream of the study area and not from location reproduction (Caspar unpubl. data). Since no data have been published on the swimming speeds of zebra mussel veligers, we assumed that the zebra mussel veligers could be modeled as passive particles in the energetic environment of the SLETZ for the following three reasons. First, veligers were observed to have an even vertical distribution in the SLETZ (Barnard et al. 2003). Second, 99.5% of the veligers observed in our study area were at the younger and smaller D-shaped stage, with

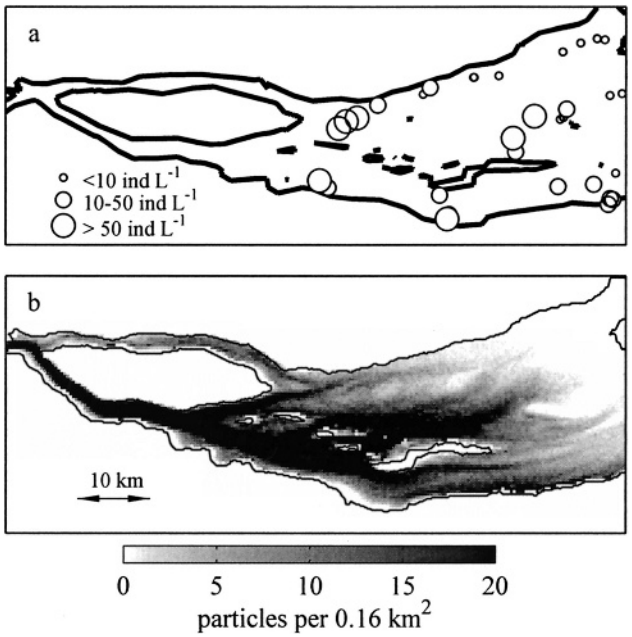

Fig. 5. Horizontal distributions of (a) zebra mussel veligers and (b) tidally averaged particles.

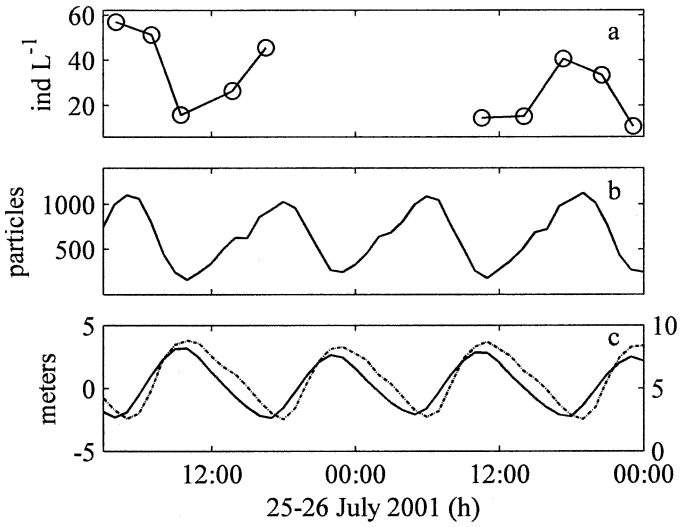

Fig. 6. Fixed point sampling results: (a) concentration of zebra mussel veligers, (b) number of particles, and (c) water level elevation (solid line and left y-axis) and salinity (dashed line and right y-axis).

a mean size of 110 μm (Winkler et al. 2005). Third, veligers have been observed to be easily damaged in turbulent environments (Horvath and Lamberti 1999).

To simulate the transport of zebra mussel veligers in the SLETZ, passive particles were introduced continuously at the release point at a rate of 20 particles per time step over the modeling period. At the release point, the particles were evenly distributed at 2-m intervals from 8 m to 46 m below the surface. Based on field data, the particles were given a salinity-dependent mortality rate, which consisted of a random 50% chance of mortality at 5 and a 100% mortality at 10 (Winkler unpubl. data). When mortality was achieved, the particles were removed from the simulation. The salinity at the particle location was calculated with trilinear interpolation. With this mortality pattern, the average time a particle spent in the SLETZ was 10 days, which was well within the larval period (Sprung 1992).

The particle results were compared to field data for zebra mussel veligers using horizontal distributions and fixed point sampling. To collect the data for the horizontal distributions, five field surveys were conducted during the summer of 2000 on 04 June, 15 June, 15 July, 28 July, and 08 August (Winkler et al. 2005). During these surveys, 12 surface stations were sampled; we sampled five in the north channel, two in the middle channel, and five in the south channel. Since each station was chosen according to salinity, the location of the stations differed with every survey depending on tidal stage. To collect the field data for the fixed point, a survey was conducted on 25–26 July 2001. During the survey, veliger samples were collected from the surface, middle, and bottom of the water column over two 12-h periods (Barnard et al. 2003).

To qualitatively compare the particle results to the field data, the horizontal near-surface distribution of veligers from the five surveys in 2000 and the tidally averaged horizontal distribution of particles are presented (Fig. 5). Ideally, a single survey should have been conducted throughout the study area in 2001 for comparing horizontal distributions; however, the surveys from 2000 provided the best available data. The tidally averaged distribution was calculated by averaging the number of particles in a 0.16-km^2 area over the last 14-d spring-neap cycle of the modeling period. The relative abundance of veligers from the surveys corresponded generally with the predicted horizontal distributions of particles. In both cases, the highest concentrations were observed in the south and middle channels. Since the field and model data came from different years and, consequently, different hydrologic conditions, a statistical comparison was not possible.

For the fixed point sampling, model results and field data were compared temporally for a single location near the north shore (Fig. 2). Since the samples showed a constant vertical distribution of veligers, they were vertically averaged for this comparison (Fig. 6a). From the model, the total number of particles was recorded at the fixed point (Fig. 6b). Water level elevations and salinity at the fixed point were calculated by the circulation model (Fig. 6c). The concentrations of zebra mussel veligers and particles at the fixed point showed excellent agreement, increasing on low tide, when the salinity was low, and decreasing on high tide, when the salinity was high. For a statistical comparison, the number of particles was plotted against the concentration of zebra mussel veligers (Fig. 7), and the correlation coefficient (r) was calculated to be 0.89. In simulations without the imposed mortality, the number of particles at the fixed point remained constant at 1,800 and did not match the observed veliger pattern.

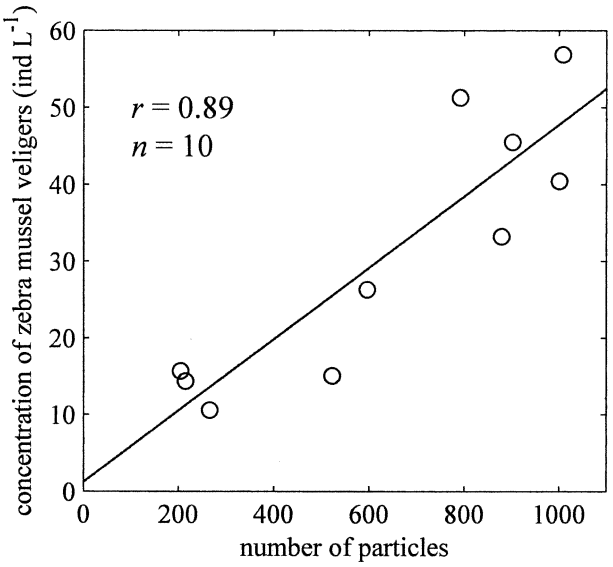

Fig. 7. Concentration of zebra mussel veligers versus number of particles for the fixed point.

Retention mechanisms

In this section, physical and biological mechanisms for zooplankton retention are evaluated using the physical–biological model. First the effect of density-driven baroclinic flow, a physical mechanism, is explored. Next, two biological mechanisms, vertical swimming and sinking and tidal vertical migration, are investigated.

Baroclinic flow—In this section, the effect of baroclinic density-driven flow on particle distributions is explored. For this experiment, passive particles with no imposed mortality were continuously released into the model at a rate of 20 particles per time step over the course of the modeling period. At this release rate, the average number of particles in the model at any one time was 150,000. Particles were introduced at the release point (Fig. 2) and were evenly distributed through the water column at 2-m intervals from 8 m to 46 m below the surface. Two simulations were run, one with baroclinic flow and one without baroclinic flow. Baroclinic flow was removed from the circulation model by setting the saline expansivity equal to zero, which removed the density effects of salinity. The saline expansivity relates salinity to density in the scalar transport scheme (Gross et al. 1999).

The tidally averaged particle distributions and the residual depth-averaged salinities were very different for the two simulations (Fig. 8). Both the tidally averaged particle distributions and the residual salinities were created by averaging in time over the last 14-d spring-neap cycle of the modeling period. When baroclinic flow was included in the simulation, large cross-estuary salinity gradients were created, and the particles concentrated in the low-salinity areas and the middle and south channels. When baroclinic flow was removed, the large cross-estuary salinity gradients disappeared, and the particles were more evenly distributed throughout the SLETZ, with the highest concentrations in the north and middle channels. Vertical particle distributions for both simulations showed an even distribution of particles throughout the water column.

Vertical swimming and sinking—In this section we explore how vertical swimming and sinking affects particle distribution and residence times. Vertical swimming and sinking was incorporated into the physical–biological model by the biological velocity, w_b, in Eq. 3. A negative biological velocity represented downward swimming or sinking, and a positive biological velocity represented upward swimming. Using the continuous particle release described in the previous section, two sets of simulations were conducted, in which all of the particles within a single

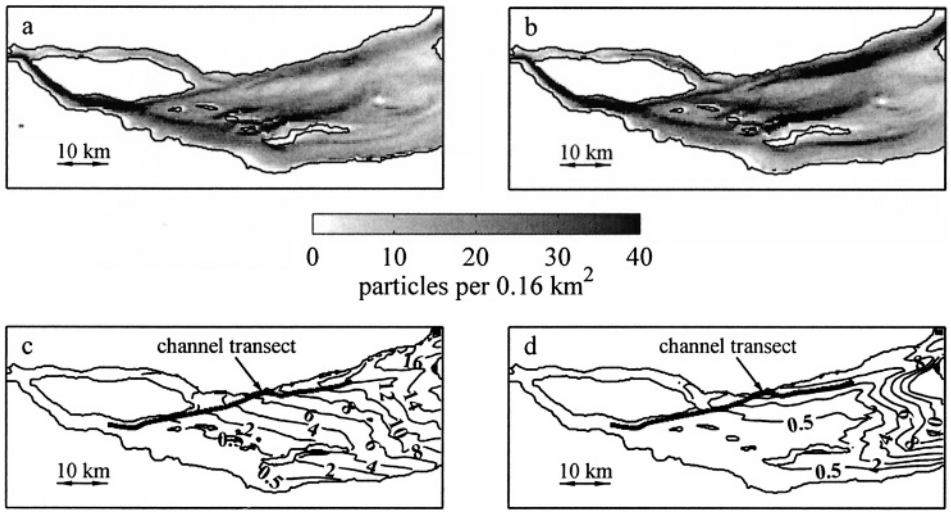

Fig. 8. Tidally averaged particle distribution (a) with baroclinic flow and (b) without baroclinic flow. Residual depth-averaged salinities (c) with baroclinic flow and (d) without baroclinic flow. The residual currents and salinities along the channel transect are shown in Fig. 10.

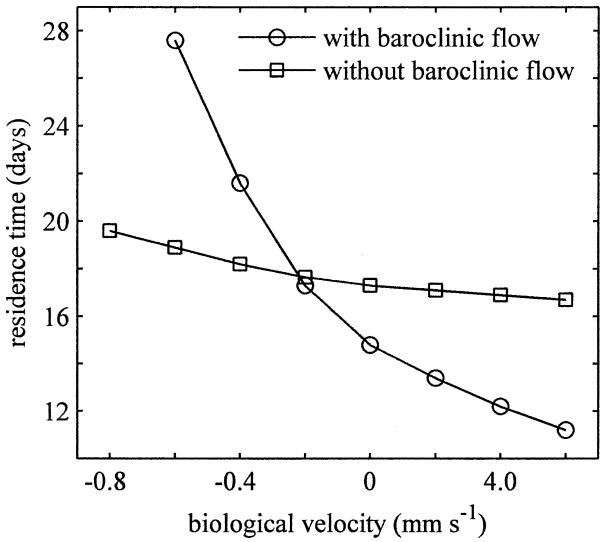

Fig. 9. Residence time versus biological velocity with baroclinic flow and without baroclinic flow.

simulation were given the same constant biological velocity. The first set of simulations included baroclinic flow and the second did not. From these simulations, residence times were calculated for biological velocities ranging from -0.8 mm s^{-1} to 0.6 mm s^{-1} using Eq. 6 (Fig. 9).

The effect of vertical particle movement on residence time was amplified in the presence of baroclinic flow (Fig. 9). For example, when the negative biological velocity or sinking speed was increased from 0.2 mm s^{-1} to 0.4 mm s^{-1}, the residence time increased by 4.3 d when baroclinic flow was present but by only 0.6 d when baroclinic flow was removed. With a negative biological velocity or sinking speed of 0.8 mm s^{-1}, the particles were 100% contained in the study area for the length of the modeling period when baroclinic flow was present, an infinite residence time. Yet when baroclinic flow was removed, the particles had a residence time of only 19.6 d.

It appears that this difference in residence times was due to gravitational circulation, a mean downstream pattern of denser water flowing beneath less-dense water (Dyer 1997). To demonstrate this, the residual currents and salinity with and without baroclinic flow were calculated along a transect (Fig. 10), which ran from south to north channels (Fig. 8c,d). The dashed line in Fig. 10a identifies the location at which the residual or mean current is zero. Produced by the circulation model, the residual currents and salinity were calculated by averaging in time over the modeling period. The difference between the residual velocity at the surface and the residual velocity at the bottom, the vertical shear, was much greater when baroclinic flow was present. As particles sank or swam down in the water column, they encountered smaller downstream or even upstream residual velocities when baroclinic flow was presented (Fig. 10a), allowing them be retained longer.

Vertical swimming and sinking also had a much greater effect on particle distribution when baroclinic flow was present. The tidally averaged horizontal particle distributions with baroclinic flow and without baroclinic flow were compared for a negative biological velocity or sinking speed of 0.6 mm s^{-1} and for a positive biological velocity or upward swimming speed of 0.6 mm s^{-1} (Fig. 11). In the

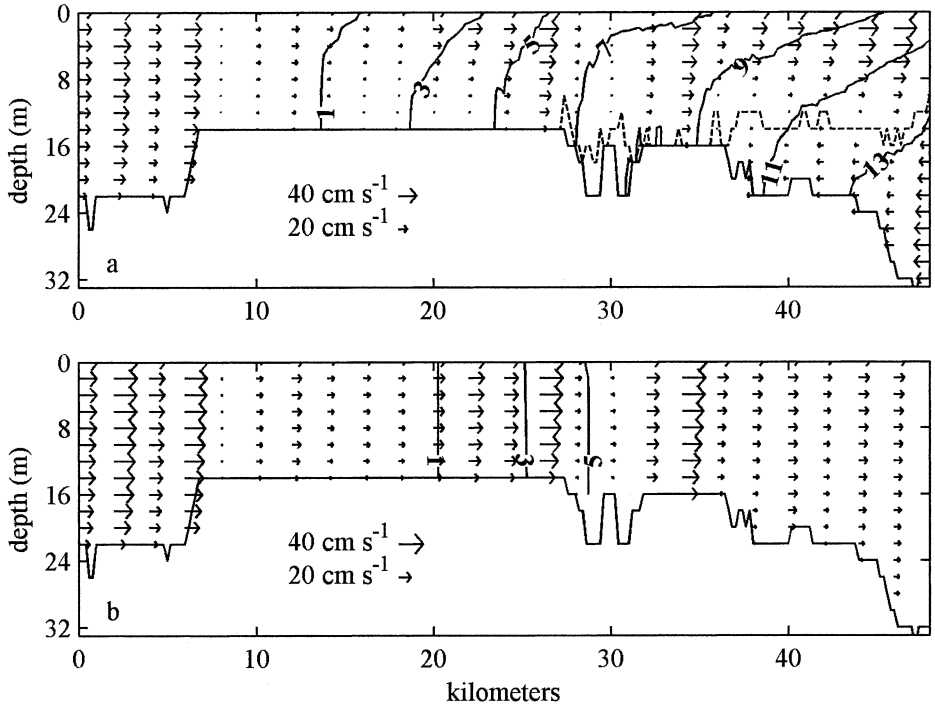

Fig. 10. Channel transect of residual currents and salinity (a) with baroclinic flow and (b) without baroclinic flow. The dashed line identifies the location at which the residual current is zero.

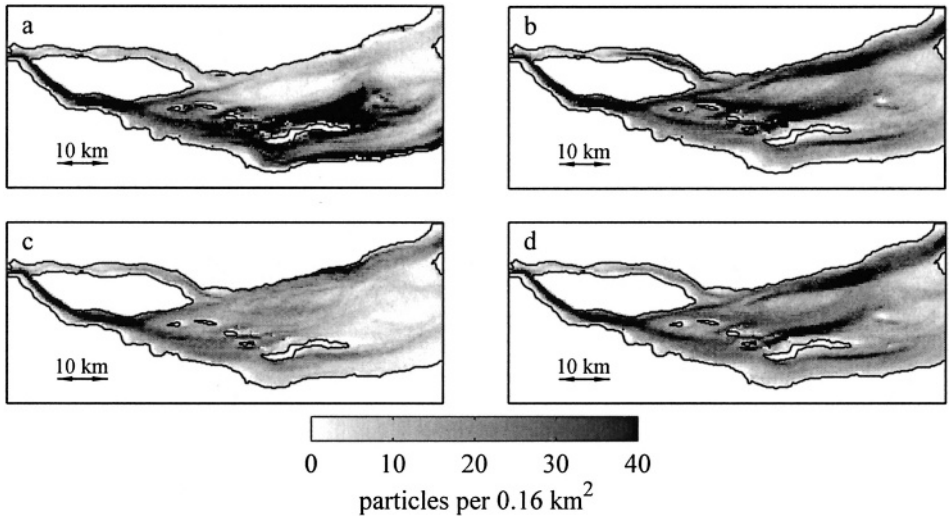

Fig. 11. Tidally averaged particle distributions: (a) sinking at 0.6 mm s^{-1} with baroclinic flow, (b) sinking at 0.6 mm s^{-1} without baroclinic flow, (c) upward swimming at 0.6 mm s^{-1} with baroclinic flow, and (d) upward swimming at 0.6 mm s^{-1} without baroclinic flow.

sinking case with baroclinic flow (Fig. 11a), the particles were mostly concentrated in the south and middle channels in the areas of low salinity. In the upward swimming case with baroclinic flow (Fig. 11c), the particles were more evenly distributed throughout the SLETZ, with the highest concentrations in the south channel downstream of Ile d'Orleans and the north shore, a very different distribution than the sinking case. In the sinking and upward swimming cases without baroclinic flow (Fig. 11b,d), the distributions were very similar, with slightly more particles in the north and middle channels in the sinking simulation.

Tidal vertical migration—To explore TVM in the SLETZ, two sets of simulations were conducted, one with baroclinic flow and one without baroclinic flow. For each simulation, 100,000 particles with no imposed mortality were introduced at the beginning of the modeling period in a single pulse at the release point (Fig. 2). When released, the particles were vertically distributed in groups of 5,000 at 2-m intervals from depths of 8 m to 46 m. For a single simulation, all particles were given the same TVM pattern, which consisted of a positive biological velocity for upward migration on flood and an equal negative biological velocity for downward migration on ebb. Each set of simulations included biological velocities, which will be termed TVM speeds, of 0.1 mm s^{-1}, 0.5 mm s^{-1}, 1 mm s^{-1}, 2 mm s^{-1}, 3 mm s^{-1}, and 10 mm s^{-1}.

We observed that a larger number of particles were retained at lower TVM speeds when baroclinic flow was present. The percent of particles retained at the end of the modeling period versus TVM speed is compared in Fig. 12. At a TVM speed of 1 mm s^{-1}, close to 100% of the particles were retained when baroclinic flow was present, while only 53% of the particles were retained when baroclinic flow was absent. For TVM speeds of 2 mm s^{-1} or greater, 100% of the particles were retained throughout the modeling period for both simulations with and without baroclinic flow.

Particle distributions at low TVM speeds were also influenced by baroclinic flow. Tidally averaged particle distributions for TVM speeds of 1 mm s^{-1} and 3 mm s^{-1} with and without baroclinic flow are shown in Fig. 13. At a TVM speed of 1 mm s^{-1}, the particles were mostly restricted to the middle channel when baroclinic flow was present, while the particles were much more spread out in the north and middle channels when baroclinic flow was no longer imposed. At a TVM speed of 3 mm s^{-1}, the particle distributions with and without baroclinic flow were practically identical. For both cases with and without

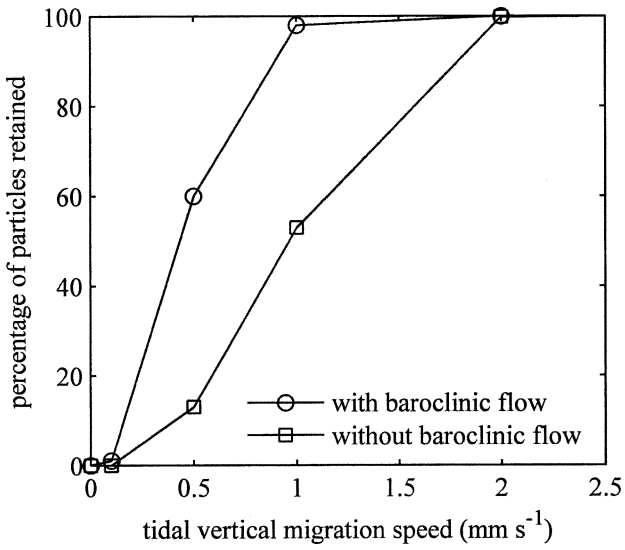

Fig. 12. Percentage of particles retained versus TVM speed with baroclinic flow and without baroclinic flow.

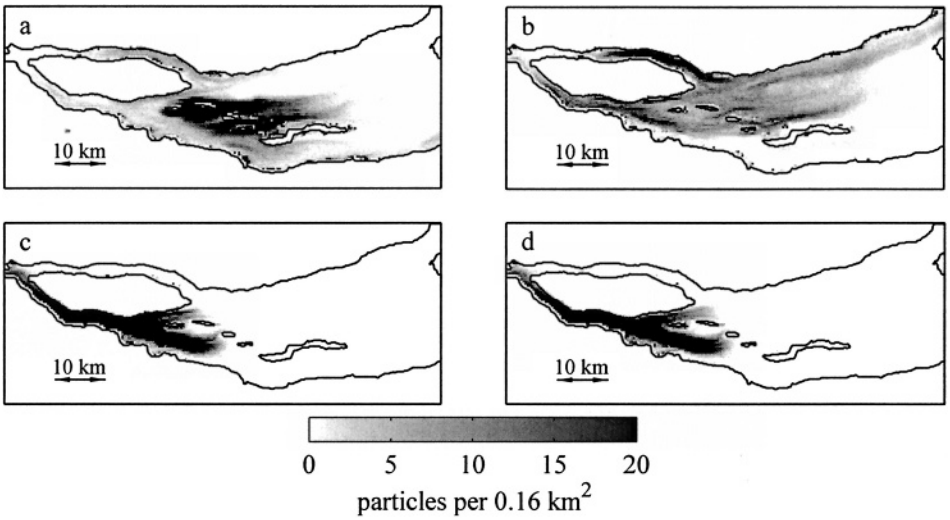

Fig. 13. Tidally averaged particle distributions for TVM speeds of (a) 1 mm s^{-1} with baroclinic flow, (b) 1 mm s^{-1} without baroclinic flow, (c) 3 mm s^{-1} with baroclinic flow, and (d) 3 mm s^{-1} without baroclinic flow.

baroclinic flow, as the TVM speed increased, the particles became more concentrated and moved further upstream into the areas of lower salinities. At a TVM speed of 10 mm s^{-1}, all of the particles were located upstream of the study area in the St. Lawrence River.

Created by the horizontal salinity gradients, baroclinic flow and gravitational circulation were determined to be a critical part of particle retention and distribution in the SLETZ. When passive particles were released into the SLETZ with and without baroclinic flow, their distribution changed dramatically, with the highest concentrations moving from the south and middle channels to the north and middle channels. The passive particle distribution with baroclinic flow was similar to the pattern of suspended sediment observed in the SLETZ (D'anglejan 1990). By comparing salinity contours to the particle distributions, it appeared that the particle pattern was related to the large cross-estuary salinity gradients, which were created in the presence of baroclinic flow.

By evaluating the influence of vertical swimming and sinking on retention with and without baroclinic flows, we discovered that small changes in vertical speed had a much greater effect on residence times when baroclinic flow was present, which was attributed to the sheared mean velocity profile of gravitational circulation. TVM, a pattern of upward migration on flood and downward migration on ebb, was found to be a viable retention mechanism for the SLETZ. At TVM speeds of less than 2 mm s^{-1}, baroclinic flow enhanced retention. As the TVM speeds increased beyond 2 mm s^{-1}, the particles became more concentrated and moved farther upstream, regardless of the presence of baroclinic flow,

Our study indicates that baroclinic flow and gravitational circulation enhance the ability of biological behaviors, such as vertical swimming and sinking and TVM, to retain zooplankton in the SLETZ. Since baroclinic density-driven flow derived from horizontal salinity gradients is a defining feature of ETZs, we believe that the amplifying effect of baroclinic flow on retention is not unique to the SLETZ, but may be an important factor in maintaining stable zooplankton assemblages in the ETZs of other riverine estuaries. For example, in San Francisco Bay a zooplankton maxima has been observed to be associated with the location of the ETZ and not with geographical location (Kimmerer et al. 1998), even though the ETZ can move over 40 km under different hydrologic conditions (Monismith et al. 2002). On the other hand, vertical migration may not be as effective for retention in estuaries in which there are no salinity gradients.

References

Ahrens, J. H., and U. Dieter. 1973. Extensions of Forsythe's method for random sampling from the normal distribution. Math Comput **27:** 927–937.

Arthur, J. A., and M. D. Ball. 1979. Factors influencing the entrapment of suspended material in the San Francisco Bay-delta estuary, p. 143–174. *In* T. J. Conomos [ed.], San Francisco Bay: The urbanized estuary: 58th Annual Meeting of the Pacific Division. American Association for the Advancement of Science.

Barnard, C., J. J. Frenette, and W. F. Vincent. 2003. Planktonic invaders of the St Lawrence estuarine transition zone: Environmental factors controlling the distribution of zebra mussel veligers. Can. J. Fish. Aquat. Sci. **60:** 1245–1257.

Bartsch, J. 1993. Application of a circulation and transport model system to the dispersal of herring larvae in the North-Sea. Cont. Shelf Res. **13:** 1335–1361.

Batchelder, H. P., C. A. Edwards, and T. M. Powell. 2002. Individual-based models of copepod populations in coastal upwelling regions: Implications of physiologically and environmentally influenced diel vertical migration on demographic success and nearshore retention. Prog. Oceanogr. **53:** 307–333.

Bousfield, E. L., G. Filteau, M. O'niell, and P. Gentes. 1975. Population dynamics of the zooplankton in the middle St Lawrence Estuary, p. 325–351. *In* L. E. Cronin [ed.], Estuarine research. Academic Press.

CASULLI, V., AND E. CATTANI. 1994. Stability, accuracy and efficiency of a semi-implicit method for 3-dimensional shallow-water flow. Comput. Math. Appl. **27:** 99–112.

———, AND R. T. CHENG. 1992. Semi-implicit finite-difference methods for 3-dimensional shallow-water flow. Int. J. Numer. Methods Fluids **15:** 629–648.

CRONIN, T. W., AND R. B. FORWARD. 1982. Tidally timed behavior: Effects on larval distribution in estuaries, p. 505–520. *In* V. S. Kennedy [ed.], Estuarine comparisons. Academic Press.

D'ANGLEJAN, B. 1990. Recent sediments and sediment transport processes in the St. Lawrence Estuary, p. 109–129. *In* M. I. El-Sabh and N. Silverberg [eds.], Oceanography of a large-scale estuarine system: The St. Lawrence. Springer-Verlag.

DAUVIN, J. C., AND J. J. DODSON. 1990. Relationship between feeding incidence and vertical and longitudinal distribution of rainbow smelt larvae (*Osmerus-mordax*) in a turbid well-mixed estuary. Mar. Ecol. Prog. Ser. **60:** 1–12.

DYER, K. R. 1997. Estuaries: A physical introduction, 2nd ed. Wiley.

EL-SABH, M. I., AND N. SILVERBERG. 1990. The St. Lawrence Estuary: Introduction, p. 1–9. *In* M. I. El-Sabh and N. Silverberg [eds.], Oceanography of a large-scale estuarine system: The St. Lawrence. Springer-Verlag.

FERZIGER, J. H. 1998. Numerical methods for engineering application, 2nd ed. Wiley.

FISCHER, H. B., E. J. LIST, R. C. Y. KOH, J. IMBERGER, AND N. H. BROOKS. 1979. Mixing in inland and coastal waters. Academic Press.

FORWARD, R. B., AND R. A. TANKERSLEY. 2001. Selective tidal-stream transport of marine animals. Oceanogr. Mar. Biol. **39:** 305–353.

GRIOCHE, A., X. HARLAY, P. KOUBBI, AND L. F. LAGO. 2000. Vertical migrations of fish larvae: Eulerian and Lagrangian observations in the Eastern English Channel. J. Plankton Res. **22:** 1813–1828.

GROSS, E. S., J. R. KOSEFF, AND S. G. MONISMITH. 1999. Three-dimensional salinity simulations of south San Francisco Bay. J. Hydraul. Eng. ASCE **125:** 1199–1209.

HANNAH, C. G., C. E. NAIMIE, J. W. LODER, AND F. E. WERNER. 1997. Upper-ocean transport mechanisms from the Gulf of Maine to Georges Bank, with implications for Calanus supply. Cont. Shelf Res. **17:** 1887–1911.

HARE, J. A., AND OTHERS. 1999. Larval transport during winter in the SABRE study area: Results of a coupled vertical behaviour three-dimensional circulation model. Fish. Oceanogr. **8:** 57–76.

HARMS, J. H., M. R. HEATH, A. D. BRYANT, J. O. BACKHAUS, AND D. A. HAINBUCHER. 2000. Modelling the Northeast Atlantic circulation: Implications for the spring invasion of shelf regions by *Calanus finmarchicus*. Ices J. Mar. Sci. **57:** 1694–1707.

HOFFMANN, E. E., AND C. M. LASCARA. 1998. Overview of interdisciplinary modeling for marine ecosystems, p. 507–540. *In* K. H. Brink and A. R. Robinson [eds.], The sea: The global coastal ocean, processes and methods. Wiley.

HORVATH, T. G., AND G. A. LAMBERTI. 1999. Mortality of zebra mussel, *Dreissena polymorpha*, veligers during downstream transport. Freshwat. Biol. **42:** 69–76.

HUNTER, J. R., P. D. CRAIG, AND H. E. PHILLIPS. 1993. On the use of random-walk models with spatially-variable diffusivity. J. Comput. Physics **106:** 366–376.

KIMMERER, W. J., J. R. BURAU, AND W. A. BENNETT. 1998. Tidally oriented vertical migration and position maintenance of zooplankton in a temperate estuary. Limnol. Oceanogr. **43:** 1697–1709.

———, ———, AND ———. 2002. Persistence of tidally-oriented vertical migration by zooplankton in a temperate estuary. Estuaries **25:** 359–371.

LAPRISE, R., AND J. J. DODSON. 1989. Ontogeny and importance of tidal vertical migrations in the retention of larval smelt *Osmerus-mordax* in a well-mixed estuary. Mar. Ecol. Prog. Ser. **55:** 101–111.

———, AND ———. 1994. Environmental variability as a factor controlling spatial patterns in distribution and species-diversity of zooplankton in the St-Lawrence-Estuary. Mar. Ecol. Prog. Ser. **107:** 67–81.

MERTZ, G., AND Y. GRATTON. 1990. Topographic waves and topographically induced motions in the St. Lawrence Estuary, p. 94–108. *In* M. I. El-Sabh and N. Silverberg [eds.], Oceanography of a large-scale estuarine system: The St. Lawrence. Springer-Verlag.

MILLER, C. B. 1983. The zooplankton of estuaries, p. 103–149. *In* B. H. Ketchum [ed.], Estuaries and enclosed seas. Elsevier.

MONISMITH, S. G., W. KIMMERER, J. R. BURAU, AND M. T. STACEY. 2002. Structure and flow-induced variability of the subtidal salinity field in northern San Francisco Bay. J. Phys. Oceanogr. **32:** 3003–3019.

MORGAN, C. A., J. R. CORDELL, AND C. A. SIMENSTAD. 1997. Sink or swim? Copepod population maintenance in the Columbia River estuarine turbidity-maxima region. Mar. Biol. **129:** 309–317.

OKUBO, A. 1986. Dynamical aspects of animal grouping: Swarms, schools, flocks, and herds. Adv. Biophys. **22:** 1–94.

ROMAN, M. R., D. V. HOLLIDAY, AND L. P. SANFORD. 2001. Temporal and spatial patterns of zooplankton in the Chesapeake Bay turbidity maximum. Mar. Ecol. Prog. Ser. **213:** 215–227.

SIMONS, R. D. 2004. Circulation and zooplankton retention in the estuarine transition zone of the St. Lawrence Estuary. Ph.D. thesis, Stanford Univ.

SPRUNG, M. 1992. The other life: An account of present knowledge of the larval phase of *Dreissena polymorpha*, p. 39–53. *In* T. F. Nalepa and D. W. Schloesser [eds.], Zebra mussels: Biology, impacts, and control. CRC Press.

THOMSON, D. J. 1984. Random-walk modeling of diffusion in inhomogeneous turbulence. Q. J. Roy. Meteorol. Soc. **110:** 1107–1120.

TREMBLAY, M. J., J. W. LODER, F. E. WERNER, C. E. NAIMIE, F. H. PAGE, AND M. M. SINCLAIR. 1994. Drift of sea scallop larvae *Placopecten-magellanicus* on Georges Bank—a model study of the roles of mean advection, larval behavior and larval origin. Deep-Sea Res. II **41:** 7–49.

VISSER, A. W. 1997. Using random walk models to simulate the vertical distribution of particles in a turbulent water column. Mar. Ecol. Prog. Ser. **158:** 275–281.

WINKLER, G., J. J. DODSON, N. BERTRAND, D. THIVIERGE, AND W. F. VINCENT. 2003. Trophic coupling across the St. Lawrence River estuarine transition zone. Mar. Ecol. Prog. Ser. **251:** 59–73.

———, P. SIROIS, L. E. JOHNSON, AND J. J. DODSON. 2005. Invasion of an estuarine transition zone by *Dreissena polymorpha* veligers has no detectable effect on zooplankton community structure. Can. J. Aquat. Fish. Sci. **62:** 578–592.

YOUNG, C. M. 1995. Behavior and locomotion during the dispersal phase of larval life, p. 249–277. *In* L. McEdward [ed.], Ecology of marine invertebrate larvae. CRC Press.

Received: 19 December 2005
Amended: 8 June 2006
Accepted: 21 June 2006